DALTON

Syntheses and characterization of binuclear Rh_2, Ir_2 and RhIr complexes containing dimethyl phosphonate and pyrazolate bridging ligands

Mauricio Valderrama,*[a] Jacqueline Cuevas,[a] Daphne Boys,[b] Daniel Carmona,*[c] M. Pilar Lamata,[d] Fernando Viguri,[d] Reinaldo Atencio,[c] Fernando J. Lahoz[c] and Luis A. Oro *[c]

[a] *Departamento de Química Inorgánica, Facultad de Química, Pontificia Universidad Católica de Chile, Casilla 306, Santiago, Chile*
[b] *Departamento de Física, Facultad de Ciencias Físicas y Matemáticas, Universidad de Chile, Casilla 487-3, Santiago, Chile*
[c] *Departamento de Química Inorgánica, Instituto de Ciencia de Materiales de Aragón, Universidad de Zaragoza-C.S.I.C., 50009 Zaragoza, Spain*
[d] *Departamento de Química Inorgánica, Escuela Universitaria de Ingeniería Técnica Industrial, Corona de Aragón 35, 50009 Zaragoza, Spain*

The reaction of $[Ir(\eta^5\text{-}C_5Me_5)I\{PO(OMe)_2\}\{P(OH)(OMe)_2\}]$ with pyrazole (Hpz) in the presence of $AgPF_6$ gave $[Ir(\eta^5\text{-}C_5Me_5)\{PO(OMe)_2\}\{P(OH)(OMe)_2\}(Hpz)]PF_6$ **1**. Deprotonation of **1** with sodium carbonate afforded the neutral compound $[Ir(\eta^5\text{-}C_5Me_5)\{PO(OMe)_2\}_2(Hpz)]$ **2** which, in turn, can be deprotonated to $[(\eta^5\text{-}C_5Me_5)Ir\{PO(OMe)_2\}_2(pz)M']$ (M′ = Tl **3** or Na **4**) by Tl(acac) (acac = acetylacetonate) or NaH, respectively. The complex $[Ir(\eta^5\text{-}C_5Me_5)I_2\{P(OH)(OMe)_2\}]$ **5**, prepared by cleaving the iodide bridges in $[\{Ir(\eta^5\text{-}C_5Me_5)I\}_2(\mu\text{-}I)_2]$ with $HPO(OMe)_2$, reacted with Hpz in the presence of $AgPF_6$ to give $[Ir(\eta^5\text{-}C_5Me_5)\{PO(OMe)_2\}(Hpz)_2]PF_6$ **6**. Complexes of formulae $[(\eta^5\text{-}C_5Me_5)Ir\{PO(OMe)_2\}_2(pz)M''L_2]$ [$M''L_2$ = $Rh(CO)_2$ **7**, Rh(cod) **8** or Ir(cod) **9**] were prepared from **2** and $[Rh(acac)(CO)_2]$ or from **3** and the appropriate $[\{M''(cod)\}_2(\mu\text{-}Cl)_2]$ dimer (cod = cycloocta-1,5-diene). Complex **6** reacted with $[\{Rh(cod)\}_2(\mu\text{-}Cl)_2]$ in basic medium to give $[(\eta^5\text{-}C_5Me_5)Ir\{PO(OMe)_2\}(pz)_2Rh(cod)]$ **10**. The rhodium–thallium compound $[(\eta^5\text{-}C_5Me_5)Rh\{PO(OMe)_2\}_2(pz)Tl]$ or the *in situ* prepared sodium derivative $[(\eta^5\text{-}C_5Me_5)Rh\{PO(OMe)_2\}(pz)_2Na]$ reacted with the dimers $[\{M''(diolefin)\}_2(\mu\text{-}Cl)_2]$ affording $[(\eta^5\text{-}C_5Me_5)Rh\{PO(OMe)_2\}_2(pz)M''(diolefin)]$ [M″(diolefin) = Ir(cod) **11** or Rh(nbd) **12**] or $[(\eta^5\text{-}C_5Me_5)\{PO(OMe)_2\}Rh(pz)_2M''(diolefin)]$ [M″(diolefin) = Rh(cod) **13**, Ir(cod) **14** or Rh(nbd) **15**], respectively (nbd = bicyclo[2.2.1]hepta-2,5-diene). Related heterovalent complexes of general formula $[I(\eta^5\text{-}C_5Me_5)M\{PO(OMe)_2\}_2M''(diolefin)]$ [M = Ir, M′(diolefin) = Rh(cod) **16** or Ir(cod) **17**; M = Rh, M″(diolefin) = Rh(cod) **18**, Ir(cod) **19**, or Rh(nbd) **20**] have been prepared starting from the mononuclear complexes $[M(\eta^5\text{-}C_5Me_5)I\{PO(OMe)_2\}\{P(OH)(OMe)_2\}]$ (M = Ir or Rh). All the complexes have been characterized by spectroscopic means and the fluxional behaviour of **7**–**9**, **11** and **12**, in solution, has been studied. The protonation of **8** by toluene-*p*-sulfonic acid is reported. The structures of **8** and **16** have been determined by X-ray diffraction methods. Both complexes consist of doubly bridged binuclear (C_5Me_5)Ir–Rh(cod) species, where the Ir atoms exhibit pseudo-octahedral co-ordination and the rhodium square planar. The bridging system in **16** is formed by two identical P,O-bonded phosphonate groups, while in **8** a pyrazolate and a phosphonate ligand are bridging the metals. The intermetallic separations are 4.0445(9) (**8**) and 4.0928(9) Å (**16**).

Bimetallic complexes containing metals in different oxidation states are of much interest due, in part, to the potential interplay of additive and co-operative effects between metal centres across a bridging ligand.[1] One useful synthetic approach to this type of compound implies the reaction of metalloligand complexes with appropriate metallic fragments. We have reported that the anionic compound $[Rh(\eta^5\text{-}C_5Me_5)I\{PO(OMe)_2\}_2]^-$ reacts as a bidentate O,O or as a tridentate O,O,I donor ligand towards a variety of metallic moieties.[2]

Taking advantage of the versatility of pyrazolates as exobidentate bridging ligands,[3] we have recently described new mononuclear anionic complexes containing a pyrazolate and two phosphonate groups $[Rh(\eta^5\text{-}C_5Me_5)\{PO(OMe)_2\}_2(pz)]^-$ which, usually, act as tridentate ligands forming a variety of homo- and hetero-binuclear complexes.[4] However, when this type of ligand is co-ordinated to rhodium(I) the resulting complex presents an interesting solution behaviour which can be accounted for by assuming a change in the hapticity from η^2 to η^3.

Following our previous studies[4] on the bridging ability of phosphonate ligands, we are now exploring the possibilities of mixed phosphonate–pyrazolate bridges to stabilize binuclear heterovalent homo- and hetero-nuclear complexes. Here we describe the preparation of the cationic mononuclear complex $[Ir(\eta^5\text{-}C_5Me_5)\{PO(OMe)_2\}\{P(OH)(OMe)_2\}(Hpz)]PF_6$, its mono- or di-deprotonated derivatives and the cationic bis(pyrazole) complex $[Ir(\eta^5\text{-}C_5Me_5)\{PO(OMe)_2\}(Hpz)_2]PF_6$. All of these mononuclear compounds can be used as starting materials to prepare a variety of binuclear species. The co-ordinative behaviour of these complexes has been studied by variable-temperature NMR spectroscopy and the molecular structures of two complexes have been determined.

Results and Discussion

Mononuclear complexes

The preparative reactions of these complexes are summarized in Scheme 1. The neutral iridium(III) complex $[Ir(\eta^5\text{-}C_5Me_5)I\{PO(OMe)_2\}\{P(OH)(OMe)_2\}]$ reacted with pyrazole (Hpz), in

$$[\mathrm{Ir}(\eta^5\text{-}\mathrm{C_5Me_5})\mathrm{I}\{\mathrm{PO(OMe)_2}\}\{\mathrm{P(OH)(OMe)_2}\}] + \mathrm{Hpz} \xrightarrow[-\mathrm{AgI}]{\mathrm{AgPF_6}} \underset{\mathbf{1}}{[\mathrm{Ir}(\eta^5\text{-}\mathrm{C_5Me_5})\{\mathrm{PO(OMe)_2}\}\{\mathrm{P(OH)(OMe)_2}\}(\mathrm{Hpz})]\mathrm{PF_6}}$$

$$\mathbf{1} + \mathrm{Na_2CO_3} \xrightarrow{\mathrm{H_2O}} \underset{\mathbf{2}}{[\mathrm{Ir}(\eta^5\text{-}\mathrm{C_5Me_5})\{\mathrm{PO(OMe)_2}\}_2(\mathrm{Hpz})]}$$

$$\mathbf{2} + \mathrm{Tl(acac)\ or\ NaH} \longrightarrow \underset{\mathrm{M'} = \mathrm{Tl}\ \mathbf{3},\ \mathrm{Na}\ \mathbf{4}}{[(\eta^5\text{-}\mathrm{C_5Me_5})\mathrm{Ir}\{\mathrm{PO(OMe)_2}\}_2(\mathrm{pz})\mathrm{M'}]}$$

$$[\{\mathrm{Ir}(\eta^5\text{-}\mathrm{C_5Me_5})\mathrm{I}\}_2(\mu\text{-}\mathrm{I_2})] + \mathrm{HPO(OMe)_2} \longrightarrow \underset{\mathbf{5}}{[\mathrm{Ir}(\eta^5\text{-}\mathrm{C_5Me_5})\mathrm{I_2}\{\mathrm{P(OH)(OMe)_2}\}]}$$

$$\mathbf{5} + \mathrm{Hpz} \xrightarrow[-\mathrm{AgI}]{\mathrm{AgPF_6}} \underset{\mathbf{6}}{[\mathrm{Ir}(\eta^5\text{-}\mathrm{C_5Me_5})\{\mathrm{PO(OMe)_2}\}(\mathrm{Hpz})_2]\mathrm{PF_6}}$$

Scheme 1

the presence of silver hexafluorophosphate, to give the cationic compound $[Ir(\eta^5\text{-}C_5Me_5)\{PO(OMe)_2\}\{P(OH)(OMe)_2\}(Hpz)]PF_6$ **1**. The hydrogen-bonded proton of the phosphonate group was neutralized by reaction with sodium carbonate to give $[Ir(\eta^5\text{-}C_5Me_5)\{PO(OMe)_2\}_2(Hpz)]$ **2** which, in turn, reacted with thallium acetylacetonate or sodium hydride rendering the corresponding neutral heterobimetallic complexes $[Ir(\eta^5\text{-}C_5Me_5)\{PO(OMe)_2\}_2(pz)M']$ (M′ = Tl **3** or Na **4**).

Complexes **1**–**4** were characterized by elemental analyses, IR and NMR spectroscopy. The IR spectra showed the presence of ν(P=O) and δ(P=O) bands as well as the ν(N–H) absorptions of the pyrazole ligand (see Experimental section). Their ^1H NMR spectra (Table 1) exhibited a triplet for the C_5Me_5 group, the characteristic pattern of two virtual triplets (with a slight difference in coupling constants) due to the presence of two pairs of non-isochronous OMe groups, and two doublets (H^3, H^5) and one pseudo-triplet (H^4) for the protons of the pyrazole or pyrazolate ligand.

Compounds **1**–**4** can be used as metalloligands through one or more of the three-atom donor set O,O,N of their phosphonate and pyrazolate groups. For co-ordinative comparative purposes, we have prepared the cationic compound $[Ir(\eta^5\text{-}C_5Me_5)\{PO(OMe)_2\}(Hpz)_2]PF_6$ **6**, in which a potential O,N,N donor set is present. Addition of $HPO(OMe)_2$ to the dimer $[\{Ir(\eta^5\text{-}C_5Me_5)I\}_2(\mu\text{-}I)_2]$ and subsequent reaction with $AgPF_6$, in the presence of pyrazole, of the intermediate compound $[Ir(\eta^5\text{-}C_5Me_5)I_2\{P(OH)(OMe)_2\}]$ **5**, afforded **6** in very good yield.

The monophosphonate complexes **5** and **6** showed, in the ^1H NMR spectra, two doublet signals for the C_5Me_5 and OMe groups and the expected two doublets and one pseudo-triplet for the protons of the pyrazole ligand (Table 1). The $^{31}P\text{-}\{^1H\}$ NMR spectra of the mononuclear complexes **1**–**6** showed the expected single resonance due to the co-ordinated phosphonate groups (see Experimental section) and, from all the experimental data, a three-legged piano-stool structure was inferred.

Binuclear complexes

We have shown the ability of complexes **2**–**4** and **6** to act as metalloligands by treating them under appropriate conditions with complexes containing the $M''L_2$ moiety [M″ = Rh or Ir; L_2 = diolefin or $(CO)_2$]. Thus, **2** can be deprotonated by the acetylacetonate compound $[Rh(acac)(CO)_2]$ giving the IrRh complex $[(\eta^5\text{-}C_5Me_5)Ir\{PO(OMe)_2\}_2(pz)Rh(CO)_2]$ **7**, the thallium cation in **3** can act as a halogen scavenger towards the dimers $[\{M''(cod)\}_2(\mu\text{-}Cl)_2]$ (M″ = Rh or Ir; cod = cycloocta-1,5-diene) affording the IrM″ complexes $[(\eta^5\text{-}C_5Me_5)Ir\{PO(OMe)_2\}_2(pz)M''(cod)]$ (M″ = Rh **8** or Ir **9**) and the reaction of complex **6** with KOH and $[\{Rh(cod)\}_2(\mu\text{-}Cl)_2]$ gave the IrRh complex $[(\eta^5\text{-}C_5Me_5)Ir\{PO(OMe)_2\}(pz)_2Rh(cod)]$ **10** (Scheme 2), most probably, *via* the non-isolated anionic intermediate $[Ir(\eta^5\text{-}C_5Me_5)\{PO(OMe)_2\}(pz)_2]^-$.

Analogously, the related rhodium complex $[(\eta^5\text{-}C_5Me_5)Rh\{PO(OMe)_2\}_2(pz)Tl]$[4b] reacted with $[\{M''(diolefin)\}_2(\mu\text{-}Cl)_2]$ rendering $[(\eta^5\text{-}C_5Me_5)Rh\{PO(OMe)_2\}_2(pz)M''(diolefin)]$ {M″(diolefin) = Ir(cod) **11** or Rh(nbd) **12** (nbd = bicyclo[2.2.1]hepta-2,5-diene)} and $[Rh(\eta^5\text{-}C_5Me_5)\{PO(OMe)_2\}(pz)(Hpz)]$[5] reacted, in the presence of sodium hydride, with the same dimers $[\{M''(diolefin)\}_2(\mu\text{-}Cl)_2]$ with abstraction of their chlorides and formation of the corresponding derivatives $[(\eta^5\text{-}C_5Me_5)\{PO(OMe)_2\}Rh(pz)_2M''(diolefin)]$ [M″(diolefin) = Rh(cod) **13**, Ir(cod) **14** or Rh(nbd) **15**].

Following similar synthetic methodologies, we have prepared the binuclear complexes $[I(\eta^5\text{-}C_5Me_5)M\{PO(OMe)_2\}_2M''(diolefin)]$ [M = Ir, M″(diolefin) = Rh(cod) **16** or Ir(cod) **17**; M = Rh, M″(diolefin) = Rh(cod) **18**, Ir(cod) **19** or Rh(nbd) **20**] with one iodide and two phosphonate anions starting from $[I(\eta^5\text{-}C_5Me_5)M\{PO(OMe)_2\}\{P(OH)(OMe)_2\}]$ and the appropriate diolefin-containing compound.

All the binuclear complexes were isolated as stable microcrystalline yellow or orange solids. Their C, H and N microanalytical data are given in the Experimental section. The IR spectrum of complex **7** in pentane solution showed two bands at 2070 and 1995 cm^{-1}, characteristic of a *cis*-dicarbonyl structure. Their ^1H NMR spectra were in good agreement with the proposed formulations showing the presence of C_5Me_5, pz, $PO(OMe)_2$ and the corresponding diolefin ligand in the required proportions. In complexes **7**–**15** the inequivalence of the three protons of the pyrazolate group is accounted for by the asymmetry of co-ordination around this heterocyclic ligand.

The existence of different bridging ligands allows a better insight into the fluxional processes that are usually undergone by rhodium(I) or iridium(I) compounds of symmetric tripodal ligands such as tris(pyrazolyl)borates or the related $[Co(\eta^5\text{-}C_5H_5)\{PO(OR)_2\}_3]$ anions. The most interesting structural information was obtained from the ^{31}P NMR spectra. At room temperature, in deuteriated chloroform, there were two types of $^{31}P\text{-}\{^1H\}$ NMR spectra: those of compounds **10** and **13**–**20** showed narrow, well resolved resonances (see Experimental section) and those of **7**–**9**, **11** and **12** (with two phosphonates and one pyrazolate ligand) consisted of broad uninformative signals (Table 2). Additionally, the spectra of the former type were essentially invariant over the range 213–333 K, whereas the modifications of the spectra of the latter on changing the temperature strongly indicated that a fluxional process was occurring. Thus, at 213 K, the spectra of **7**–**9** consisted of two

Table 1 Proton NMR[a] chemical shifts (δ) and coupling constants (Hz) of complexes **1**–**20**

Complex	C_5Me_5 [^4J(PH)]	OMe [^3J(PH)]	Pyrazole or pyrazolate [^3J($H^{3,5}$,H^4)]			
			$H^{3/5}$	$H^{5/3}$	H^4	Other
1	1.7 (t) [3.1]	3.7 (vt) [11.8] 3.9 (vt) [11.1]	8.0 (d) [2.7]	7.7 (d) [1.9]	6.4 (pt)	9.2 (s, br, NH) 11.2 (s, br, POH)
2	1.7 (t) [3.1]	3.4 (vt) [11.5] 3.6 (vt) [11.3]	7.5 (d) [2.3]	7.6 (d) [1.6]	6.3 (pt)	14.0 (s, vbr, NH)
3	1.6 (t) [2.8]	3.6 (vt) [11.3] 3.7 (vt) [11.0]	7.4 (d) [1.7]	7.6 (d) [1.7]	6.2 (pt)	—
4	1.6 (t) [2.6]	3.5 (vt) [11.3] 3.6 (vt) [11.0]	7.6 (d) [1.7]	7.5 (d) [1.6]	6.2 (pt)	—
5	2.0 (d) [3.4]	3.8 (d) [11.6]	—	—	—	4.4 (s, br, POH)
6[b]	1.7 (d) [3.1]	3.6 (d) [11.3]	8.0 (d) [2.7]	7.8 (d) [2.2]	6.6 (pt)	14.0 (s, br, NH)
7	1.8 (t) [2.8]	3.4 (d) [11.2] 3.6 (d) [11.4]	8.0 (d) [2.1]	7.4 (d) [2.2]	6.2 (pt)	—
8	1.8 (t) [2.7]	3.5 (d) [11.1] 3.5 (d) [11.4]	8.0 (d) [2.0]	6.9 (d) [2.2]	6.0 (pt)	1.9 (m, 4 H, CH_2),[c] 2.6 (m, 4 H, CH_2), 4.0 (br s, 4 H, CH=CH)
9	1.8 (t) [2.7]	3.4 (d) [11.3] 3.5 (d) [11.0]	8.0 (d) [2.0]	7.2 (d) [2.1]	6.1 (pt)	1.5 (m, 4 H, CH_2), 2.3 (m, 4 H, CH_2), 3.7 (br s, 4 H, CH=CH)
10	1.7 (d) [2.8]	3.0 (d) [11.3]	7.9 (d) [1.7]	7.4 (d) [1.8]	6.1 (pt)	1.8 (m, 4 H, CH_2),[c] 2.5 (m, 2 H, CH_2), 2.6 (m, 2 H, CH_2), 3.8 (br s, 2 H, CH=CH), 4.4 (br s, 2 H, CH=CH)
11	1.7(t) [4.0]	3.4 (vt) [11.1] 3.6 (vt) [11.3]	8.0 (d) [1.9]	7.3 (d) [2.0]	6.1 (pt)	1.5 (m, 4 H, CH_2), 2.3 (m, 4 H, CH_2), 3.7 (br s, 4 H, CH=CH)
12	1.8 (t) [3.9]	3.5 (vt) [11.1] 3.6 (vt) [11.3]	7.8 (d) [1.9]	6.6 (d) [2.0]	6.1 (pt)	1.3 (s, 2 H, CH), 3.7 (br s, 4 H, CH=CH), 3.8 (br s, 2 H, CH_2)
13	1.7 (d) [4.1]	2.9 (d) [10.9]	7.8 (d) [1.9]	7.5 (d) [1.9]	6.1 (pt)	1.9 (br s, 4 H, CH_2), 2.5 (m, 4 H, CH_2), 3.8 (br s, 2 H, CH=CH), 4.4 (br s, 2 H, CH=CH)
14	1.7 (d) [4.2]	3.0 (d) [10.9]	7.9 (d) [1.8]	7.5 (d) [1.9]	6.1 (pt)	1.7 (m, 4 H, CH_2),[c] 2.4 (m, 4 H, CH_2), 3.5 (br s, 2 H, CH=CH), 4.1 (br s, 2 H, CH=CH)
15	1.6 (d) [4.1]	3.1 (d) [10.9]	7.8 (d) [1.5]	7.0 (d) [1.2]	6.1 (pt)	1.4 (br s, 2 H, CH), 3.8 (m, 4 H, CH=CH), 4.0 (br s, 2 H, CH_2)
16	1.8 (t) [2.7]	3.4 (vt) [11.1] 3.5 (vt) [11.2]	—	—	—	1.5 (m, 4 H, CH_2), 2.5 (m, 4 H, CH_2), 3.7 (br s, 4 H, CH=CH)
17	1.9 (t) [2.7]	3.5 (vt) [11.1] 3.6 (vt) [11.2]	—	—	—	1.9 (m, 4 H, CH_2), 2.3 (m, 4 H, CH_2), 3.6 (br s, 4 H, CH=CH)
18	1.8 (t) [3.9]	3.5 (vt) [11.0] 3.6 (vt) [11.2]	—	—	—	1.5 (m, 4 H, CH_2), 2.5 (m, 4 H, CH_2), 3.7 (br s, 4 H, CH=CH)
19	1.9 (t) [3.9]	3.5 (vt) [11.1] 3.6 (vt) [11.3]	—	—	—	1.2 (m, 4 H, CH_2), 2.3 (m, 4 H, CH_2), 3.6 (br s, 4 H, CH=CH)
20	1.8 (t) [3.8]	3.4 (vt) [11.1] 3.5 (vt) [11.3]	—	—	—	0.9 (s, 2 H, CH), 3.4 (s, 4 H, CH=CH),[d] 3.7 (br s, 2 H, CH_2)

[a] Measured in $CDCl_3$ at room temperature; chemicals shifts relative to $SiMe_4$ as internal standard; s = singlet, d = doublet, t = triplet, vt = virtual triplet, pt = pseudo-triplet, m = multiplet, br = broad, vbr = very broad. [b] In $(CD_3)_2CO$. [c] Masked by the C_5Me_5 group. [d] Masked by the OMe groups.

sharp doublets, centred at about δ 43 and 59, with a ^2J(PP) coupling constant of *ca.* 70 Hz, corresponding to two phosphorus nuclei with different chemical environments. Although the high-temperature-limiting spectra of **7**–**9** were not achieved, at 373 K, in toluene, the spectra only showed a broad singlet. Similarly, at 213 K, those of **11** and **12** consisted of two sharp double doublets, due to Rh–P and P–P couplings, centred at δ 88.2 and 111.7 and 89.4 and 115.8, respectively. Again, the two inequivalent phosphorus nuclei were significantly different, their resonances being separated, one from the other, by more than 20 ppm. The high-temperature-limiting spectrum of complex **12** was achieved and, at 373 K, consisted of one sharp doublet centred at δ 96.0 with ^1J(RhP) 184.3 Hz. For **11**, a broad doublet, centred at δ 100, with ^1J(RhP) 192.9 Hz, was observed at this temperature. All the experimental data can be accounted for by assuming that, in the ground state, complexes **7**–**9**, **11** and **12** have a binuclear M^{III}–M^{I} structure in which pseudo-octahedral and square-planar environments are bridged by one pyrazolate and one phosphonate, the remaining phosphonate ligand being terminal, *i.e.* only co-ordinated to the metal(III) centre. When the temperature was increased the terminal and bridging phosphonate groups exchanged, this process becoming, in general, fast at 373 K. From the equilibration of the phosphorus nuclei, the free energy of activation, $\Delta G^‡$ at the coalescence temperature, for the interconversion has been calculated (Table 2).

On the other hand, compounds **10** and **13**–**20** were stereochemically rigid in the range 213–313 K and their structures most probably consist of binuclear pseudo-octahedral metal(III) and square-planar metal(I) centres bridged by two pyrazolate (**10**, **13**–**15**) or two phosphonate groups (**16**–**20**). The remaining phosphonate or iodide group is probably only co-ordinated to the metal(III) centre.

In all cases the higher-field resonances were assigned to terminal phosphonate groups, assuming that co-ordination through the oxygen produces a deshielding of the phosphorus nucleus. When co-ordinated to rhodium(III), terminal phosphonate phosphorus resonated in the range δ 83.4–89.8, whereas bridging phosphonate phosphorus occurred at δ 103.5–115.6. Similarly, for phosphonate groups co-ordinated to iridium(III), for a terminal ligand, δ 42.5–45.1 and for bridging phosphonate groups, δ 54.35–59.5. Complexes **10** and **13**–**15**, which contained only terminal phosphonate groups, and **16**–**20**, with only bridging phosphonates, confirmed this assumption.

In order to determine the molecular structure in the solid state of these types of complexes and to gain additional information on the molecular parameters of the bridging ligands two diffractometric studies on single crystals of **8** and **16** were undertaken.

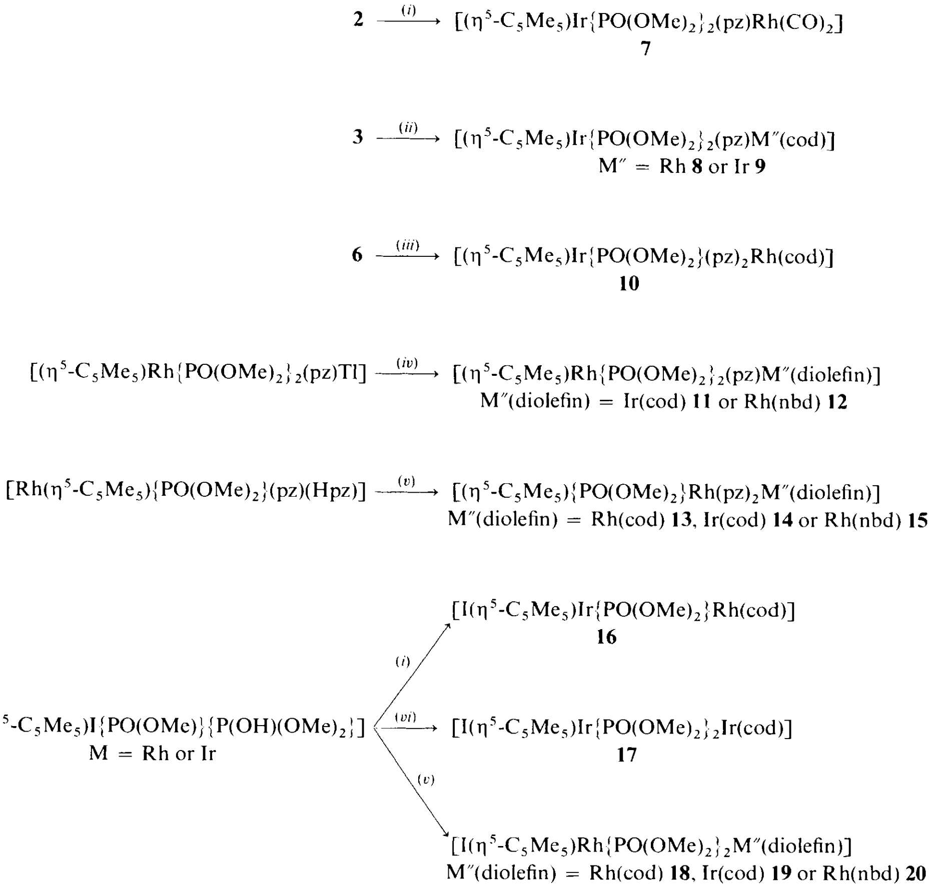

Scheme 2 (*i*) $[Rh(acac)(CO)_2]$, −Hacac; (*ii*) $\frac{1}{2}[\{M''(cod)\}_2(\mu\text{-}Cl)_2]$, −TlCl; (*iii*) $\frac{1}{2}[\{Rh(cod)\}_2(\mu\text{-}Cl)_2]$, KOH, −KCl; (*iv*) $\frac{1}{2}[\{M''(diolefin)\}_2(\mu\text{-}Cl)_2]$, −TlCl; (*v*) $\frac{1}{2}[\{M''(diolefin)\}_2(\mu\text{-}Cl)_2]$, NaH, −NaCl, $-H_2$; (*vi*) $\frac{1}{2}[\{Ir(cod)\}_2(\mu\text{-}Cl)_2]$, Tl(acac), −TlCl, −Hacac

Table 2 The $^{31}P\text{-}\{^1H\}$ NMR[a] chemical shifts (δ) and coupling constants (Hz) in $CDCl_3$ for the $PO(OMe)_2$ groups of the binuclear complexes **7**–**9**, **11** and **12**

Complex	373[b]	333	293	273	243	213 K	$\Delta G^‡$/kJ mol^{-1}
7	47.5 (br s)	42 (br s)	50 (br s)	Coalescence	41 (br d) 60 (br d)	42.5 (d) 59.5 (d) ^2J(PP) = 69.0	48.4
8	48.1 (br s)	49 (br s)	Coalescence	41 (vbr s) 59 (vbr s)	42.4 (d) 58.6 (d) ^2J(PP) = 70.0	43.2 (d) 58.1 (d) ^2J(PP) = 69.9	52.5
9	48 (vbr s)	Coalescence	42 (br s) 58 (br s)	42.0 (d) 58.3 (d) ^2J(PP) = 67.3	42.8 (d) 58.0 (d) ^2J(PP) = 69.8	43.8 (d) 57.5 (d) ^2J(PP) = 70.1	60.2
11[c]	100 (br d) ^1J(RhP) = 192.9	94 (br s)	88 (vbr s) 107 (vbr s)	87 (m) 107 (m)		88.2 (dd) ^1J(RhP) = 170.2 111.7 (dd) ^1J(RhP) = 199.8, ^2J(PP) = 93.8	54.7
12	96.0 (d) ^1J(RhP) = 184.3	99 (br d)	100 (br s)	Coalescence	89 (m) 115 (m)	89.4 (dd) ^1J(RhP) = 178.1 115.8 (dd) ^1J(RhP) = 193.1, ^2J(PP) = 87.8	47.5

[a] Chemical shifts relative to 85% H_3PO_4 in D_2O as external standard; P_t = terminal phosphorus, P_b = bridging phosphorus. [b] In $[^2H_8]$toluene. [c] Coalescence temperature: 311 K.

Molecular structures of complexes 8 and 16

The X-ray diffraction study of complex **8** reveals the presence in the unit cell of two enantiomers differing in the chirality at the iridium centre. Fig. 1 displays the molecular structure of the complex R_{Ir}-**8**[6] and Fig. 2 that of complex **16**, with the atom labelling used. The most relevant bond angles and distances for both molecules are given in Table 3. The complexes are heterodinuclear with an iridium and a rhodium atom connected by one phosphonate and one pyrazolate group (**8**) or by two phosphonates (**16**). In both cases the phosphonate anions are co-ordinated to the iridium through the phosphorus and to the rhodium through the oxygen atoms. The iridium–rhodium separations, 4.0445(9) (**8**) and 4.0928(9) Å (**16**), exclude any significant intermetallic interaction. An η^5-co-ordinated pentamethylcyclopentadienyl ligand and a terminal phosphonate group (**8**) or an iodide ligand (**16**) complete the pseudo-octahedral co-ordination of the iridium atoms. The slightly distorted square-planar co-ordination exhibited by the rhodium metals is completed, in both cases, by the two double bonds of a

Table 3 Selected bond distances (Å) and angles (°) for the complexes **8** and **16**

	8	**16**		**8**	**16**
Ir–P(1)	2.249(2)	2.253(2)	Rh–O(1)	2.076(5)	2.105(5)
Ir–P(2)	2.274(2)	2.255(2)	Rh–N(2)/O(4)[b]	2.135(7)	2.097(5)
Ir–N(1)/I[a]	2.088(5)	2.691(1)	Rh–C(15)	2.111(8)	2.087(9)
Ir–C(5)	2.270(7)	2.192(9)	Rh–C(16)	2.121(7)	2.061(8)
Ir–C(6)	2.277(6)	2.264(9)	Rh–C(19)	2.117(9)	2.073(7)
Ir–C(7)	2.250(7)	2.262(9)	Rh–C(20)	2.133(9)	2.071(7)
Ir–C(8)	2.252(6)	2.276(8)	Rh–M(1)[c]	2.001(8)	1.955(9)
Ir–C(9)	2.209(6)	2.253(7)	Rh–M(2)[c]	2.005(9)	1.955(7)
P(1)–O(1)	1.513(6)	1.511(5)	P(2)–O(4)	1.482(6)	1.510(5)
P(1)–O(2)	1.599(6)	1.612(6)	P(2)–O(5)	1.607(4)	1.586(8)
P(1)–O(3)	1.588(5)	1.606(7)	P(2)–O(6)	1.635(7)	1.590(6)
			N(1)–N(2)	1.376(8)	
P(1)–Ir–P(2)	92.3(1)	89.1(1)	O(1)–Rh–N(2)/O(4)[b]	94.5(2)	89.6(2)
P(1)–Ir–N(1)/I[a]	87.4(2)	90.9(1)	O(1)–Rh–M(1)[c]	172.0(3)	177.0(3)
P(1)–Ir–G[d]	126.3(2)	127.4(3)	O(1)–Rh–M(2)	84.6(3)	90.8(3)
P(2)–Ir–N(1)/I[a]	92.5(2)	90.3(1)	N(2)/O(4)[b]–Rh–M(1)	93.3(3)	90.7(3)
P(2)–Ir–G[d]	124.5(2)	127.1(3)	N(2)/O(4)[b]–Rh–M(2)	177.2(3)	176.3(2)
N(1)/I[a]–Ir–G[d]	123.3(3)	121.0(3)	M(1)–Rh–M(2)	87.6(3)	88.6(3)
Ir–P(1)–O(1)	112.4(2)	121.8(2)	Ir–P(2)–O(4)	117.8(2)	122.4(2)
Ir–P(1)–O(2)	115.1(2)	111.7(2)	Ir–P(2)–O(5)	114.9(2)	112.7(3)
Ir–P(1)–O(3)	113.8(2)	107.2(2)	Ir–P(2)–O(6)	104.7(2)	106.1(3)
O(1)–P(1)–O(2)	101.4(3)	106.4(3)	O(4)–P(2)–O(5)	109.7(3)	106.5(3)
O(1)–P(1)–O(3)	109.3(3)	109.5(3)	O(4)–P(2)–O(6)	109.0(3)	108.6(3)
O(2)–P(1)–O(3)	103.8(3)	97.7(3)	O(5)–P(2)–O(6)	98.8(3)	97.8(4)
Rh–O(1)–P(1)	128.5(3)	130.9(3)	Rh–O(4)–P(2)		130.5(3)
Ir–N(1)–N(2)	127.1(4)		Rh–N(2)–N(1)	130.4(4)	

[a] Bond distances and angle involving N(1) (complex **8**) or I (**16**). [b] Bond distances and angle involving N(2) in complex **8** and O(4) in **16**. [c] M(1) and M(2) represent the midpoints of the olefinic C(15)–C(16) and C(19)–C(20) bonds in both complexes **8** and **16**. [d] G represents the centroid of the η^5-C_5Me_5 ligand in complexes **8** and **16**.

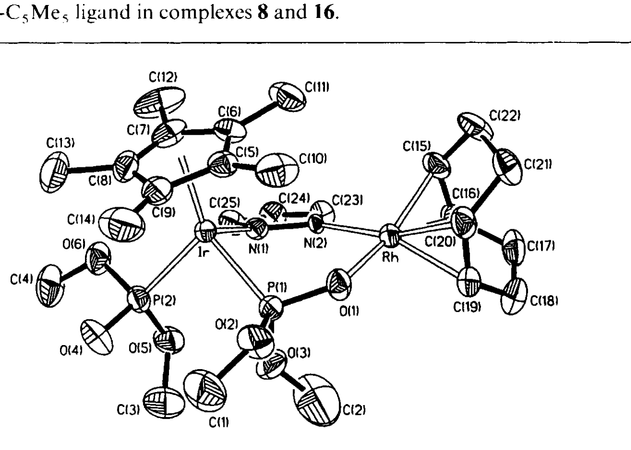

Fig. 1 Molecular structure of complex **8** with the atom-labelling scheme used. Hydrogen atoms have been omitted for clarity

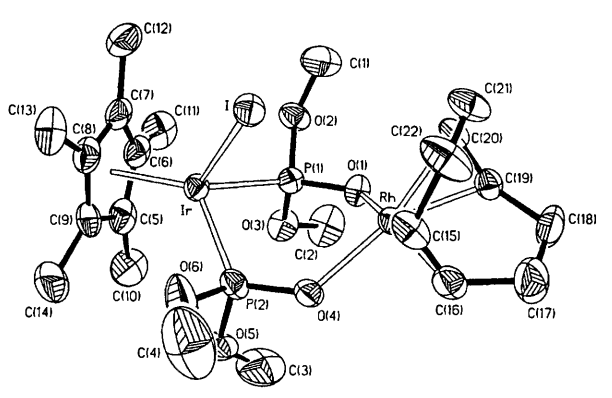

Fig. 2 Molecular representation of complex **16** with the numbering scheme used. Hydrogen atoms are omitted for clarity

chelate cyclooctadiene ligand. The deviations from the square-planar co-ordination mean planes are less than 0.060(7) (**8**) or 0.059(1) Å (**16**).

The Ir–C (ring) distances range from 2.209(6) to 2.277(6) Å for complex **8**, and from 2.192(9) to 2.276(8) Å for **16**, and are slightly longer than those usually found in pentamethylcyclopentadienyliridium(III) compounds.[7] In both cases one of these distances is significantly shorter [C(9) in **8**, and C(5) in **16**] than the remainder, which are practically equal within error (see Table 3). Additionally, the four carbon atoms bonded to the iridium at longer distances are strictly coplanar within 0.008(7) Å, with the fifth carbon bent towards the iridium by 0.072(7) (**8**) or 0.080(9) Å (**16**). Thus, the cyclopentadienyl rings adopt envelope conformations being folded by 4.9(4) (**8**) or 5.4(6)° (**16**). These features are consistent with some degree of electron-density localization in the C_5 ring towards a 'di-π-olefin-σ' bonding.[7a,8] The distribution of the internal C–C bond distances in the C_5Me_5 rings seems to verify this [two shorter distances, C(5)–C(6) and C(7)–C(8) in **8** and C(6)–C(7) and C(8)–C(9) in **16**, and three longer ones], although the differences in them are within the accuracy limits. Interestingly, analogous differences in the M–C (ring) bond distances (around 0.05 Å), and similar folding angles of the five-membered rings (range 4.2–6.8°), to those observed in **8** and **16** have been reported in related complexes where an 'η^4-diene:η^1-yl' co-ordination mode has been confirmed.[8] As usual, the methyl substituents are bent away from the iridium atom [deviation 0.028(8)–0.255(9) (**8**) and 0.058(10)–0.223(10) Å (**16**)].

The bridging Ir–P(1) bond distance in complex **8**, 2.249(2) Å, is similar to those in **16**, 2.253(2) and 2.255(2) Å, and compares well with those found in related iridium(III) compounds with bridging phosphonate ligands[9] such as $[\{(\eta^5\text{-}C_5Me_5)Ir(\mu\text{-}Cl)[\mu\text{-}PO(OMe)_2]_2\}_2Ni]$ [2.263(3) and 2.260(3) Å], $[\{(\eta^5\text{-}C_5Me_5)ClIr[\mu\text{-}PO(OMe)_2]_2\}_2M]$ [M = Cu, 2.260(3) and 2.264(3); M = Pb, 2.248(5), 2.251(3), 2.240(5) and 2.252(5) Å] or with the closely related rhodium cationic complex $[(\eta^5\text{-}C_5Me_5)Rh\{\mu\text{-}PO(OMe)_2\}_2(\mu\text{-}pz)Ru(C_6H_6)]^+$ [2.243(3) and 2.235(3) Å].[4a] The terminal Ir–P(2) distance, 2.274(2) Å, is slightly longer than the bridging ones.

The Rh–O(1) bond distance in complex **8**, 2.076(5) Å, is similar to the values found for $[Pd\{(\mu\text{-}Cl)[\mu\text{-}PO(OMe)]_2Rh\text{-}$

(cod)}][10] [2.076 and 2.085(3) Å] and is slightly shorter than those found for **16**, 2.105(5) and 2.097(5) Å. The bridging phosphoryl P–O bond distances, 1.513(6) Å (**8**) and 1.511(5) and 1.510(5) Å (**16**), are equal, and longer than the terminal unco-ordinated P(2)–O(4) distance, 1.482(6) Å, in **8**. As observed in related trinuclear IrNiIr, IrCuIr, IrPbIr,[9] RhTlRh,[2] RhPdRh[10] or RuCuRu[11] and heterodinuclear RhRu[4] complexes [mean co-ordinated P–O bond length 1.519(5) Å], the phosphoryl P–O group suffers a feeble elongation upon co-ordination, likely as a consequence of the electron density release from the oxygen towards the second metal, but it maintains clear double-bond character [mean unco-ordinated P–O bond length 1.507(5) Å].[12] As a point of reference, the single bond P–OMe distances average 1.607(3) Å in **8** and 1.599(4) Å in **16**.

In both complexes the cyclooctadiene molecules adopt the usual boat conformation observed when this group acts as a chelating ligand. The four Rh–C (olefinic) bond distances are identical within each complex, but the values differ significantly from **8** [2.120(5) Å] to **16** [2.073(5) Å]. It is worth noting that the values observed for the Rh–C bond distances as well as for the olefinic C=C bonds in **16**, average 1.377(10) Å [and to a lesser extent in **8**, average 1.393(7) Å], are both surprisingly in the *lower* part of the range reported for square-planar rhodium(I) complexes containing the 'Rh(cod)' unit.[12] This situation is anomalous as the usual description of a metal–olefin bond involving d_π–π^* metal–olefin back donation would imply *opposite* variations of these related bond distances, M–C and C=C, with short metal–olefin distances being associated with long C=C bonds. This behaviour has been also found in the related complex $[Pd\{(\mu-Cl)[\mu-PO(OMe)_2]Rh(cod)\}_2]$,[10] where a chloride and an oxygen atom of a bridging phosphonate group are bonded *trans* to a cyclooctadiene molecule, and has been explained as due to the high electronegativity of these atoms (Cl and O) which forces the cyclooctadiene to co-ordinate through strong σ and weak π components.

The Ir–N(1) bond distance in complex **8**, 2.088(5) Å, compares well with other bridging pyrazolate Ir–N bond distances, 2.098(10) and 2.065(11) Å for $[\{Ir(\eta^5-C_5Me_5)\}_2(\mu-H)_2(\mu-pz)]BF_4$,[7c] 2.090(8) and 2.098(10) Å for $[(\eta^5-C_5Me_5)Ir(\mu-pz)_2(\mu-CO)Ir(CO)(dppen)]\ BPh_4$[7g] (dppen = $Ph_2PCHCHPPh_2$) and 2.095(8) Å for $[\eta^5-C_5Me_5)Ir(\mu-pz)(\mu-I)_2Rh(CO_2Me)I(CO)]$,[7e] and is slightly longer than those found in the iridium–silver compound $[(\eta^5-C_5Me_5)(pz)Ir(\mu-pz)_2Ag(PPh_3)]$ [2.073(3) and 2.075(3) Å].[7f] The Rh–N(2) bond length is comparable to those found in other rhodium(I) pyrazolate complexes.[13]

The Ir–I separation, 2.691(1) Å, in complex **16** is similar to those found in related complexes containing the '$(\eta^5-C_5Me_5)IrI$' moiety, as in the dinuclear species $[\{Ir(\eta^5-C_5Me_5)I\}_2(\mu-I)_2]$ [average 2.689(1) Å][7a,14] and $[\{Ir(\eta^5-C_5Me_5)I\}_2(\mu-I)(\mu-NO)]$ [average 2.679(10) Å],[15] or in the mononuclear complex $[Ir(\eta^5-C_5Me_5)I_2(CNC_6H_3Me_2-2,6]$ [2.701(1) Å].[16]

The reaction of complex **8**, in deuteriated chloroform, with equimolar amounts of toluene-*p*-sulfonic acid, monitored by ^{31}P NMR spectroscopy at 213 K, showed that the two sharp doublets at δ 43.2 and 58.1 from the starting material decreased and a singlet at δ 54.0 emerged. This reactivity can be explained assuming that protonation takes place at the nitrogen of the pyrazolate bridging ligand which becomes terminal [only co-ordinated to the metal(III) centre]. Subsequently, the terminal phosphonate ligand co-ordinates to M^I, forming the cationic species $[(\eta^5-C_5Me_5)Ir\{\mu-PO(OMe)_2\}_2(Hpz)Rh(cod)]^+$.

In summary, in the ground state, only two of the three anionic potentially bridging groups present in the new binuclear complexes reported are acting as bridging ligands. The priority order to behave as a bridging ligand is pz > phosphonate > iodide. In this type of compound the chemical shift of the phosphorus nucleus of the phosphonate ligand could be used as a reliable diagnostic for its bridging or terminal nature. Thus, terminal phosphonate ligand resonances appeared shifted about 15 ppm to higher field than the corresponding bridging ones, for iridium(III) compounds, and about 25 ppm for related rhodium(III) derivatives. Finally, protonation of complex **8** which contains bridging pyrazolate and bridging and terminal phosphonate groups occurs preferentially at one of the nitrogens of the pyrazolate ligand instead of at the oxygen of the phosphonate groups. The protonated pyrazolate group exchanges its bridging position with that of the terminal phosphonate ligand.

Experimental

All reactions were carried out under purified nitrogen by using Schlenk-tube techniques. Solvents were dried, distilled and stored under a nitrogen atmosphere. The starting materials $[Ir(\eta^5-C_5Me_5)I\{PO(OMe)_2\}\{P(OH)(OMe)_2\}]$,[17] $[\{Ir(\eta^5-C_5Me_5)I\}_2(\mu-I)_2]$,[18] $[Rh(acac)(CO)_2]$,[19] $[\{M''(cod)\}_2(\mu-Cl)_2]$ (M″ = Rh[20] or Ir[21]) $[\{Rh(nbd)\}_2(\mu-Cl)_2]$,[22] $[(\eta^5-C_5Me_5)Rh\{PO(OMe)_2\}_2(pz)Tl]$,[4b] $[Rh(\eta^5-C_5Me_5)\{PO(OMe)_2\}(Hpz)(pz)]$,[5] $[Rh(\eta^5-C_5Me_5)\{PO(OMe)_2\}\{P(OH)(OMe)_2\}]$[2] and $[Rh(acac)(cod)]$[20] were prepared according to reported methods. Infrared spectra were recorded on a Perkin-Elmer 567 spectrophotometer (range 4000–200 cm^{-1}). Elemental analyses (C, H and N) were determined using a Perkin-Elmer 240C microanalyser. The NMR spectra were recorded on Bruker AC200 and Varian XL-200 spectrometers, chemical shifts being relative to $SiMe_4$ (^1H) and 85% H_3PO_4 in D_2O (^{31}P) as internal and external standards, respectively. Molar conductivities were measured in *ca.* 5 × 10^{-4} mol dm^{-3} acetone solutions using a WtW LF-521 conductimeter.

Preparation of complexes

$[Ir(\eta^5-C_5Me_5)\{PO(OMe)_2\}\{P(OH)(OMe)_2\}(Hpz)]PF_6$ 1. A solution of $[Ir(\eta^5-C_5Me_5)I\{PO(OMe)_2\}\{P(OH)(OMe)_2\}]$ (300.0 mg, 0.45 mmol) in Me_2CO (20 cm^3) was treated with $AgPF_6$ (114.1 mg, 0.45 mmol) and Hpz (30.6 mg, 0.45 mmol). The resulting mixture was boiled under reflux for 14 h in the absence of light. The AgI formed was filtered off through Kieselguhr and the solution obtained concentrated under reduced pressure to a small volume (*ca.* 1 cm^3). Slow diffusion of Et_2O gave white needles, which were filtered off, washed with Et_2O and air-dried. Yield: 306.5 mg, 90% (Found: C, 26.8; H, 4.3; N, 3.5. $C_{17}H_{32}F_6IrN_2O_6P_3$ requires C, 26.9; H, 4.25; N, 3.7%). $\tilde{\nu}_{max}/cm^{-1}$ (KBr) 3320 (NH); 1130 and 605 (PO); 850 and 560 (PF_6^-). $\delta_P(CDCl_3)$ 58.2 (s). Λ_M = 137 $ohm^{-1}\ cm^2\ mol^{-1}$.

$[Ir(\eta^5-C_5Me_5)\{PO(OMe)_2\}_2(Hpz)]$ 2. To an aqueous solution of complex **1** (200.2 mg, 0.26 mmol) was added an excess of Na_2CO_3 (106.0 mg, 1.0 mmol). The solution was extracted with $CHCl_3$ (2 × 10 cm^3) and the organic layer was dried with anhydrous $MgSO_4$. After filtration, the resulting solution was evaporated to dryness and the residue dissolved in Et_2O. Evaporation of the solvent gave a pale yellow oil, which was solidified to a white-cream solid by addition of pentane. Yield: 87.3 mg, 54% (Found: C, 33.5; H, 5.2; N, 4.4. $C_{17}H_{31}IrN_2O_6P_2$ requires C, 33.3; H, 5.1; N, 4.6%). $\tilde{\nu}_{max}/cm^{-1}$ (KBr) 3360 (NH); 1110 and 600 (PO). $\delta_P(CDCl_3)$ 43.8 (s).

$[(\eta^5-C_5Me_5)Ir\{PO(OMe)_2\}_2(pz)Tl]$ 3. A mixture of complex **2** (100.3 mg, 0.16 mmol) and the stoichiometric amount of Tl(acac) (49.5 mg, 0.16 mmol) in Me_2CO (15 cm^3) was stirred at room temperature for 1 h. The solution was filtered and evaporated to dryness. The residue was dissolved in the minimum volume of pentane. White crystals were obtained by cooling the solution to −25 °C. Yield: 101.2 mg, 76% (Found: C, 24.8; H, 3.6; N, 3.3. $C_{17}H_{30}IrN_2O_6P_2Tl$ requires C, 25.0; H, 3.7; N, 3.4%). $\tilde{\nu}_{max}/cm^{-1}$ (KBr) 1127 and 594 (PO). $\delta_P(CDCl_3)$ 45.7 (s).

$[(\eta^5\text{-}C_5Me_5)Ir\{PO(OMe)_2\}_2(pz)Na]$ 4. Addition of a slight excess of NaH (7.2 mg, dispersion in mineral oil, 80% w/w, 0.22 mmol) to a solution of complex **2** (122.7 mg, 0.20 mmol) in anhydrous tetrahydrofuran (thf) (10 cm^3) produced immediate evolution of hydrogen. The resulting suspension was stirred until the evolution of hydrogen ceased and the excess of NaH was filtered off. The solution was evaporated to dryness. A white solid was obtained from the residue by stirring it with pentane. Yield: 84.3 mg, 66% (Found: C, 32.4; H, 4.85; N, 4.5. $C_{17}H_{30}IrN_2NaO_6P_2$ requires C, 32.1; H, 4.8; N, 4.4%). $\tilde{\nu}_{max}$/cm^{-1} (KBr) 1125 and 595 (PO). δ_P(CDCl$_3$) 44.9 (s).

$[Ir(\eta^5\text{-}C_5Me_5)I_2\{P(OH)(OMe)_2\}]$ 5. A suspension of the dimer $[\{Ir(\eta^5\text{-}C_5Me_5)I\}_2(\mu\text{-}I)_2]$ (450.2 mg, 0.39 mmol) and HPO(OMe)$_2$ (110.1 mg, 1.00 mmol) in CHCl$_3$ (10 cm^3) was stirred at room temperature for 12 h. It changed from orange to dark red and was evaporated to a small volume (*ca.* 1 cm^3). A red solid precipitated upon subsequent addition of pentane. The complex was recrystallized from CHCl$_3$–pentane. Yield: 482.3 mg, 90% (Found: C, 20.8; H, 3.4. $C_{14}H_{27}I_2IrO_6P_2$: C, 20.85; H, 3.2%). $\tilde{\nu}_{max}$/cm^{-1} (KBr) 1015 and 1050 (PO). δ_P(CDCl$_3$) 70.2 (s).

$[Ir(\eta^5\text{-}C_5Me_5)\{PO(OMe)_2\}(Hpz)_2]PF_6$ 6. To a solution of complex **5** (200.7 mg, 0.29 mmol) in Me$_2$CO (20 cm^3) was added AgPF$_6$ (146.6 mg, 0.58 mmol) and Hpz (39.5 mg, 0.58 mmol). The mixture was stirred for 1 h in the absence of light and the AgI formed was filtered off through Kieselguhr. The solution obtained was concentrated to a small volume (*ca.* 1 cm^3) under reduced pressure and slow addition of Et$_2$O gave a microcrystalline yellow solid. Yield: 186.2 mg, 89% (Found: C, 30.4; H, 4.3; N, 8.0. $C_{18}H_{29}F_6IrN_2O_6P_3$: C, 30.1; H, 4.1; N, 7.8%). $\tilde{\nu}_{max}$/cm^{-1} (KBr) 3215 (NH); 1127 and 600 (PO); 850 and 560 (PF$_6^-$). δ_P[(CD$_3$)$_2$CO] 53.5 (s). Λ_M = 131 ohm^{-1} cm^2 mol^{-1}.

$[(\eta^5\text{-}C_5Me_5)Ir\{PO(OMe)_2\}_2(pz)Rh(CO)_2]$ 7. To a solution of complex **2** (123.4 mg, 0.20 mmol) in CH$_2$Cl$_2$ (10 cm^3) was added a stoichiometric amount of [Rh(acac)(CO)$_2$] (52.0 mg, 0.20 mmol). The solution was stirred at room temperature for 1 h and then evaporated to dryness. The residue was dissolved in the minimum volume of Et$_2$O and the complex precipitated by addition of pentane and cooling at −25 °C. Yield: 100.2 mg, 65% (Found: C, 29.7; H, 3.9; N, 3.6. $C_{19}H_{30}IrN_2O_8P_2Rh$ requires C, 29.6; H, 3.9; N, 3.6%). $\tilde{\nu}_{max}$/cm^{-1} (pentane) 2070 and 1995 (CO).

$[(\eta^5\text{-}C_5Me_5)Ir\{PO(OMe)_2\}_2(pz)M''(cod)]$ (M″ = Rh 8 or Ir 9). To a solution of complex **3** (163.4 mg, 0.20 mmol) in CH$_2$Cl$_2$ (10 cm^3) was added the corresponding binuclear complex $[\{M''(cod)\}_2(\mu\text{-}Cl)_2]$ (0.10 mmol). The mixture was stirred for 24 h at room temperature and then filtered through Kieselguhr (to eliminate the TlCl formed). The resulting solution was vacuum-evaporated to dryness and the residue solidified by addition of pentane and cooling to −25 °C. Complex **8**: yield, 118.0 mg, 72% (Found: C, 36.3; H, 5.2; N, 3.3. $C_{25}H_{42}IrN_2O_6P_2Rh$ requires C, 36.5; H, 5.1; N, 3.4%); $\tilde{\nu}_{max}$/cm^{-1} (KBr) 1145 and 590 (PO). Complex **9**: yield, 160.2 mg, 88% (Found: C, 32.9; H, 4.6; N, 3.1. $C_{25}H_{42}Ir_2N_2O_6P_2$ requires C, 32.9; H, 4.7; N, 3.1%). $\tilde{\nu}_{max}$/cm^{-1} (KBr) 1140 and 590 (PO).

$[(\eta^5\text{-}C_5Me_5)Ir\{PO(OMe)_2\}(pz)_2Rh(cod)]$ 10. To a suspension of complex **6** (143.5 mg, 0.20 mmol) in MeOH (10 cm^3) was added a methanolic solution of KOH (23.6 mg, 0.42 mmol) and solid $[\{Rh(cod)\}_2(\mu\text{-}Cl)_2]$ (51.7 mg, 0.10 mmol). The mixture was stirred at room temperature for 4 h and evaporated to a small volume (*ca.* 2 cm^3). Addition of pentane gave yellow crystals, which were filtered off, washed with pentane and air dried. Yield: 81.2 mg, 74% (Found: C, 40.4; H, 5.6; N, 6.9. $C_{26}H_{39}IrN_4O_3PRh$ requires C, 40.0; H, 5.0; N, 7.2%). $\tilde{\nu}_{max}$/cm^{-1} (Nujol) 1145 and 590 (PO). δ_P(CDCl$_3$) 45.1 (s).

$[(\eta^5\text{-}C_5Me_5)Rh\{PO(OMe)_2\}_2(pz)M''(diolefin)]$
[M″(diolefin) = Ir(cod) 11 or Rh(nbd) 12. To a solution of $[(\eta^5\text{-}C_5Me_5)Rh\{PO(OMe)_2\}_2(pz)Tl]$ (600.1 mg, 0.825 mmol) in C$_6$H$_6$ (10 cm^3) was added the corresponding binuclear complex $[\{M''(diolefin)\}_2(\mu\text{-}Cl)_2]$ (0.41 mmol). The mixture was stirred at 50 °C for 18 h and the TlCl formed was filtered off through Kieselguhr. The solution was evaporated to dryness under reduced pressure. The residue was dissolved in CCl$_4$ and chromatographed on Kieselgel (HF$_{254}$, type 60). The fraction eluted with CCl$_4$–Et$_2$O (1 : 1) was evaporated to a small volume and the addition of pentane caused the precipitation of a yellow solid which was filtered off, washed with pentane and air-dried. Complex **11**: yield, 410.2 mg, 60% (Found: C, 36.45; H, 5.45; N, 3.4. $C_{25}H_{42}IrN_2O_6P_2Rh$ requires C, 36.45; H, 5.1; N, 3.4%); $\tilde{\nu}_{max}$/cm^{-1} (KBr) 1180 and 600 (PO). Complex **12**: yield, 333.2 mg, 56% (Found: C, 40.4; H, 5.7; N, 3.95. $C_{24}H_{38}N_2O_6P_2Rh_2$ requires C, 40.1; H, 5.3; N, 3.9%); $\tilde{\nu}_{max}$/cm^{-1} (KBr) 1185 and 600 (PO).

$[(\eta^5\text{-}C_5Me_5)\{PO(OMe)_2\}Rh(pz)_2M''(diolefin)]$
[M″(diolefin) = Rh(cod) 13, Ir(cod) 14 or Rh(nbd) 15]. At 0 °C a slight excess of NaH (17.0 mg, dispersion in mineral oil, 80% w/w, 0.54 mmol) was added to a solution of $[Rh(\eta^5\text{-}C_5Me_5)\{PO(OMe)_2\}(pz)(Hpz)]$ (250.3 mg, 0.52 mmol) in thf or 1,2-dimethoxyethane (10 cm^3). The mixture was stirred until the evolution of hydrogen ceased and the excess of NaH was filtered off through Kieselguhr. The yellow solution obtained was evaporated to dryness at 0 °C and the residue dissolved in C$_6$H$_6$ (10 cm^3). To this solution the corresponding dimer $[\{M''(diolefin)\}_2(\mu\text{-}Cl)_2]$ (0.26 mmol) was added and the mixture stirred at room temperature for 18 h. The solution was evaporated to dryness and the residue dissolved in the minimum volume of CCl$_4$ [complex **14** was dissolved in CH$_2$Cl$_2$–CHCl$_3$ (1 : 1)] and chromatographed on Kieselgel (HF$_{254}$, type 60) using CCl$_4$–CHCl$_3$ (1 : 1) as eluent [for **14** CH$_2$Cl$_2$–Et$_2$O (1 : 1) was used]. The solution obtained was kept at 0 °C and evaporated to a small volume (*ca.* 1 cm^3). A yellow solid was precipitated by adding pentane, which was filtered off, washed with pentane and air-dried. Complex **13**: yield, 268.3 mg, 75% (Found: C, 45.4; H, 5.7; N, 8.2. $C_{26}H_{39}N_4O_3PRh_2$ requires C, 45.1; H, 5.6; N, 8.1%); $\tilde{\nu}_{max}$/cm^{-1} (KBr) 1150 and 570 (PO); δ_P(CDCl$_3$) 83.4 [d, ^1J(RhP) = 167.9 Hz]. Complex **14**: yield, 299.5 mg, 73% (Found: C, 39.9; H, 5.1; N, 7.1. $C_{26}H_{39}IrN_4O_3PRh$ requires C, 40.0; H, 5.0; N, 7.2%); $\tilde{\nu}_{max}$/cm^{-1} (KBr) 1155 and 595 (PO); δ_P(CDCl$_3$) 83.85 [d, ^1J(RhP) = 168.0 Hz]. Complex **15**: yield, 208.1 mg, 60% (Found: C, 44.3; H, 5.4; N, 8.2. $C_{25}H_{35}N_4O_3PRh_2$ requires C, 44.4; H, 5.2; N, 8.3%); $\tilde{\nu}_{max}$/cm^{-1} (KBr) 1175 and 590 (PO); δ_P(CDCl$_3$) 84.4 [d, ^1J(RhP) = 169.7 Hz].

$[I(\eta^5\text{-}C_5Me_5)Ir\{PO(OMe)_2\}_2M''(cod)]$ (M″ = Rh 16 or Ir 17. To a solution of $[Ir(\eta^5\text{-}C_5Me_5)I\{PO(OMe)_2\}\{P(OH)(OMe)_2\}]$ (135.1 mg, 0.20 mmol) in CH$_2$Cl$_2$ (10 cm^3) was added the stoichiometric amount of [Rh(acac)(cod)] (62.0 mg, 0.20 mmol). The solution was stirred at room temperature for 2 h and then evaporated to dryness. The residue was solidified by adding pentane. Yield 130.1 mg, 74% (Found: C, 30.1; H, 4.9. $C_{22}H_{39}IIrO_6P_2Rh$ **16** requires C, 30.0; H, 4.45%). $\tilde{\nu}_{max}$/cm^{-1} (KBr) 1095 and 605 (PO). δ_P(CDCl$_3$) 54.35 [d, ^2J(RhP) = 3.4 Hz].

To a solution of $[Ir(\eta^5\text{-}C_5Me_5)I\{PO(OMe)_2\}\{P(OH)(OMe)_2\}]$ (135.1 mg, 0.20 mmol) in CH$_2$Cl$_2$ (10 cm^3) was added Tl(acac) (61.0 mg, 0.20 mmol). The solution was stirred at room temperature for 1 h and evaporated to dryness. The solid residue was dissolved in CHCl$_3$–CH$_2$Cl$_2$ (1 : 1), treated with $[\{Ir(cod)\}_2(\mu\text{-}Cl)_2]$ (134.3 mg, 0.20 mmol) and the resulting solution stirred for 2 h. The mixture was filtered,

Table 4 Crystallographic data for complexes **8**·0.5CH$_2$Cl$_2$ and **16**

Complex	**8**	**16**
Formula	$C_{25}H_{42}IrN_2O_6P_2Rh \cdot 0.5CH_2Cl_2$	$C_{22}H_{39}IIrO_6P_2Rh$
M	866.1	883.5
Crystal habit	Yellow transparent prismatic	Orange irregular block
Crystal dimensions/mm	0.095 × 0.072 × 0.399	0.17 × 0.24 × 0.18
Space group	$P\bar{1}$, Triclinic	$P2_1/n$, Monoclinic
a/Å	8.666(1)	15.177(3)
b/Å	13.561(2)	10.432(2)
c/Å	14.158(1)	18.637(3)
α/°	103.760(6)	
β/°	90.261(5)	105.10(2)
γ/°	107.956(6)	
U/Å^3	1531.9(3)	2848.9(10)
Cell parameters from	68 Reflections ($20 \leqslant 2\theta \leqslant 40°$)	25 Reflections ($20 \leqslant 2\theta \leqslant 45°$)
Z	2	4
D_c/g cm^{-3}	1.878	2.060
μ/mm^{-1}	5.11	6.475
Minimum and maximum transmission	0.341, 0.595	0.068, 0.099
2θ Range/°	3–50	3–55
No. measured reflections	6588	6951
No. unique reflections (R_{int})	5395 (0.0179)	6585 (0.0284)
No. observed reflections [$F_o > 4.0\sigma(F_o)$]	4540	4148
No. parameters	350	298
R^a (observed data)	0.0324	0.0346
R'^b	0.0389	0.0332
Goodness of fit	1.14	1.08
Residual density/e Å^{-3}	1.41, −0.97	0.68, −1.31

[a] $R = (\Sigma|F_o - F_c|/\Sigma|F_o|)$. [b] $R' = [\Sigma w(F_o - F_c)^2/\Sigma wF_o^2]^{\frac{1}{2}}$, with $w^{-1} = [\sigma^2(F_o) + gF_o^2]$, where g is 0.0005 and 0.0002 for complexes **8** and **16**, respectively.

evaporated to dryness and the residue extracted with the minimum volume of Et$_2$O. Yellow crystals were obtained by cooling the solution to −25 °C, which were filtered off, washed with cold Et$_2$O and air-dried. Yield: 94.5 mg, 59% (Found: C, 27.3; H, 4.2. $C_{22}H_{39}IIr_2O_6P_2$ **17** requires C, 27.2; H, 4.0%). $\tilde{\nu}_{max}$/cm^{-1} (KBr) 1115 and 600 (PO). δ_P(CDCl$_3$) 56.0 (s).

[I(η^5-C$_5$Me$_5$)Rh{PO(OMe)$_2$}$_2$M″(diolefin)] [M″(diolefin) = Rh(cod) 18, Ir(cod) 19 or Rh(nbd) 20]. To a solution of [Rh(η^5-C$_5$Me$_5$)I{PO(OMe)$_2$}{P(OH)(OMe)$_2$}] (300.5 mg, 0.51 mmol) in thf (10 cm^3) was added a slight excess of NaH (18.2 mg, dispersion in mineral oil, 80% w/w, 0.57 mmol). The mixture was stirred until the evolution of hydrogen ceased and the excess of NaH was filtered off through Kieselguhr. The red solution obtained was evaporated to dryness and the residue dissolved in C$_6$H$_6$ (10 cm^3). To the resulting solution was added the corresponding dimer [{M″(diolefin)}$_2$(μ-Cl)$_2$] (0.25 mmol). The mixture was stirred at room temperature for 18 h in the absence of light and the NaCl formed was filtered off. The solution was evaporated to a small volume and chromatographed on Kieselgel (HF$_{254}$, type 60) using CHCl$_3$–CH$_2$Cl$_2$ (1 : 1) as eluent. Orange crystals were obtained from CHCl$_3$–hexane. Complex **18**: yield, 313.2 mg, 74% (Found: C, 33.3; H, 5.0. $C_{22}H_{39}IO_6P_2Rh_2$ requires C, 33.3; H, 4.9%); $\tilde{\nu}_{max}$/cm^{-1} (KBr) 1175 and 600 (PO); δ_P(CDCl$_3$) 103.9 [d, ^1J(RhP) = 185.2 Hz]. Complex **19**: yield, 300.7 mg, 66% (Found: C, 30.0; H, 4.6. $C_{22}H_{39}IIrO_6P_2Rh$ requires C, 29.3; H, 4.4%); $\tilde{\nu}_{max}$/cm^{-1} (KBr) 1175 and 610 (PO); δ_P(CDCl$_3$) 104.7 [d, ^1J(RhP) = 185.6 Hz]. Complex **20**: yield, 345.4 mg, 87% (Found: C, 32.65; H, 4.5. $C_{21}H_{35}IO_6P_2Rh_2$ requires C, 32.4; H, 4.5%); $\tilde{\nu}_{max}$/cm^{-1} (KBr) 1170 and 600 (PO); δ_P(CDCl$_3$) 103.5 [d, ^1J(RhP) = 184.3 Hz].

Crystallography

The crystal data and refinement parameters are summarized in Table 4. Crystals suitable for X-ray diffraction studies were obtained from chloroform–hexane (complex **8**) or dichloromethane–hexane solutions (**16**). In both cases, the selected crystals were glued onto the tip of a glass fibre. A set of randomly searched reflections was indexed to the corresponding crystal symmetry and accurate unit-cell dimensions determined by least-squares refinement. Data were collected at room temperature on a Stoe AED (**8**) or Siemens R3m/V diffractometer (**16**), with graphite-monochromated Mo-Kα radiation (λ = 0.710 73 Å) by the ω–2θ scan method. Three orientation and intensity standards were monitored throughout data collection; no variation was observed. All data were corrected for absorption using a semiempirical method (ψ scan).[23] Both structures were solved by Patterson methods (SHELXTL PLUS)[24] and conventional Fourier techniques. All non-hydrogen atoms were refined anisotropically and the hydrogen atoms included in the last cycles of refinement in observed or calculated positions, and refined riding on their carbon atoms. The structures were refined by full-matrix least squares. The refinement was based on F values and the function minimized was $\Sigma[w(F_o - F_c)^2]$ with the weight defined as $w^{-1} = [\sigma^2(F_o) + gF_o^2]$. Atomic scattering factors, corrected for anomalous dispersion for metals, I and P atoms, were used as implemented in the refinement program.[24]

Atomic coordinates, thermal parameters and bond lengths and angles have been deposited at the Cambridge Crystallographic Data Centre (CCDC). See Instructions for Authors, *J. Chem. Soc., Dalton Trans.*, 1996, Issue 1. Any request to the CCDC for this material should quote the full literature citation and the reference number 186/100.

Acknowledgements

We thank the Fondo de Desarrollo Científico y Tecnológico, Chile (Grant 460/93), Fundación Andes, Chile, the Instituto de Cooperación Iberoamericano, Spain, and the Dirección General de Investigación Científica y Técnica, Spain (Grant 92/0019), for financial support. R. A. thanks the Consejo Nacional de Investigaciones Científicas y Technólogicas, Venezuela for a grant.

References

1 C. Creutz, *Prog. Inorg. Chem.*, 1983, **30**, 1; M. A. Esteruelas, M. P. Garcia, A. M. López and L. A. Oro, *Organometallics*, 1991, **10**, 127; 1992, **11**, 702.

2 M. Valderrama, M. Scotti, P. Campos, H. Werner and G. Müller, *Chem. Ber.*, 1990, **123**, 1005.

3 S. Trofimenko, *Prog. Inorg. Chem.*, 1986, **34**, 115; D. Carmona, J. Ferrer, F. J. Lahoz, L. A. Oro, J. Reyes and M. Esteban, *J. Chem. Soc., Dalton Trans.*, 1991, 2811 and refs. therein; D. Carmona, J. Ferrer, A. Mendoza, F. J. Lahoz, L. A. Oro, F. Viguri and J. Reyes, *Organometallics*, 1995, **14**, 2066 and refs. therein.

4 (*a*) M. Valderrama, M. Scotti, J. Cuevas, D. Carmona, M. P. Lamata, J. Reyes, F. J. Lahoz, E. Oñate and L. A. Oro, *J. Chem. Soc., Dalton Trans.*, 1992, 2735; (*b*) M. Valderrama, M. Scotti and J. Cuevas, *Bol. Soc. Chil. Quim.*, 1990, **35**, 317.

5 M. Scotti, M. Valderrama and R. López, unpublished work.

6 K. Stanley and M. C. Baird, *J. Am. Chem. Soc.*, 1975, **97**, 6598; T. E. Sloan, *Top. Stereochem.*, 1981, **12**, 1.

7 (*a*) M. R. Churchill and S. A. Julis, *Inorg. Chem.*, 1979, **18**, 1215; (*b*) A. Nutton, P. M. Bailey and P. M. Maitlis, *J. Chem. Soc., Dalton Trans.*, 1981, 1997; (*c*) L. A. Oro, D. Carmona, M. P. Puebla, M. P. Lamata, C. Foces-Foces and F. H. Cano, *Inorg. Chim. Acta*, 1986, **112**, L11; (*d*) D. Carmona, L. A. Oro, M. P. Lamata, J. Elguero, M. C. Apreda, C. Foces-Foces and F. H. Cano, *Angew. Chem., Int. Ed. Engl.*, 1986, **25**, 1114; (*e*) D. Carmona, F. J. Lahoz, L. A. Oro, J. Reyes and M. P. Lamata, *J. Chem. Soc., Dalton Trans.*, 1990, 3551; (*f*) D. Carmona, F. J. Lahoz, L. A. Oro, M. P. Lamata and S. Buzarra, *Organometallics*, 1991, **10**, 3123; (*g*) D. Carmona, J. Ferrer, F. J. Lahoz, L. A. Oro, J. Reyes and M. Esteban, *J. Chem. Soc., Dalton Trans.*, 1991, 2811.

8 A. S. Batsanov and Yu. T. Struchkov, *J. Organomet. Chem.*, 1984, **265**, 305.

9 P. Campos, Ph.D. Thesis, Pontificia Universidad Católica de Chile, 1993.

10 M. Valderrama, F. J. Lahoz, L. A. Oro and F. J. Plou, *Inorg. Chim. Acta*, 1988, **150**, 157.

11 G. A. van Albada, R. A. G. de Graaf, R. Hage, J. Reedijk, E. Buchholz and W. Kläui, *Polyhedron*, 1991, **10**, 1091.

12 F. H. Allen, J. E. Davies, J. J. Galloy, O. Johnson, O. Kennard, C. F. Macrae, E. M. Mitchell, G. F. Mitchell, J. M. Smith and D. G. Watson, *J. Chem. Inf. Comput. Sci.*, 1991, **31**, 187.

13 R. Usón, L. A. Oro, M. A. Ciriano, M. T. Pinillos, A. Tiripicchio and M. Tiripicchio-Camellini, *J. Organomet. Chem.*, 1981, **205**, 247; R. Usón, L. A. Oro, M. A. Ciriano, D. Carmona, A. Tiripicchio and M. Tiripicchio-Camellini, *J. Organomet. Chem.*, 1982, **224**, 69; L. A. Oro, D. Carmona, P. L. Pérez, M. Esteban, A. Tiripicchio and M. Tiripicchio-Camellini, *J. Chem. Soc., Dalton Trans.*, 1985, 973.

14 A. Millan, P. M. Bailey and P. M. Maitlis, *J. Chem. Soc., Dalton Trans.*, 1982, 73.

15 R. J. Batchelor, F. W. B. Einstein, N. D. Lowe, B. A. Palm, X. Yan and D. Sutton, *Organometallics*, 1994, **13**, 2041.

16 W. D. Jones, R. P. Duttweiler, jun. and F. J. Jeher, *Inorg. Chem.*, 1990, **29**, 1505.

17 M. Valderrama and P. Campos, unpublished work.

18 P. M. Maitlis, *Acc. Chem. Res.*, 1978, **11**, 301.

19 Yu. S. Varsharvskii and T. G. Cherkasova, *Russ. J. Inorg. Chem.*, 1967, 599.

20 J. Chatt and L. M. Venanzi, *J. Chem. Soc.*, 1957, 4735.

21 J. L. Herde, J. C. Lambert and C. V. Senoff, *Inorg. Synth.*, 1974, **15**, 18.

22 E. W. Abel, M. A. Bennett and G. Wilkinson, *J. Chem. Soc.*, 1959, 3178.

23 A. C. T. North, D. C. Phillips and F. S. Mathews, *Acta Crystallogr., Sect. A*, 1968, **24**, 351.

24 G. M. Sheldrick, SHELXTL PLUS, Siemens Analytical X-Ray Instruments, Madison, WI, 1990.

Received 19*th February* 1996; *Paper* 6/01212D